

Theoretical Study of the Diels–Alder Reactions between Singlet ($^1\Delta_g$) Oxygen and Acenes

Siu-Hung Chien, Mei-Fun Cheng, Kai-Chung Lau, and Wai-Ke Li*

Department of Chemistry, The Chinese University of Hong Kong, Shatin, N.T., Hong Kong

Received: January 17, 2005; In Final Form: July 1, 2005

The G3(MP2) method has been employed to study the 1,4-addition reactions between singlet oxygen and five acenes, including benzene, naphthalene, anthracene, tetracene, and pentacene. In all, nine pathways between O_2 and the five acenes have been investigated. Our calculated results indicate that all nine pathways are concerted and exothermic and that the most reactive sites on the acenes are the center ring's meso-carbons. In addition, reactivity increases along the series benzene < naphthalene < anthracene < tetracene < pentacene. This trend is identical to that of aromaticity for the five acenes. A correlation between reactivity and aromaticity is briefly rationalized with natural bond orbital (NBO) analysis and frontier molecular orbital (FMO) analysis. Furthermore, some experimental kinetics data from the literature supporting the calculated results are cited.

Introduction

Acenes form a class of highly aromatic compounds. The reactivity of these compounds is a topic of intense interest.^{1–7} A reactivity trend among the acenes is that the reactivity of an acene increases with the number of rings in the acene molecule. Some theoretical studies^{1,2,5,8} attempted to explain this trend by earlier models, including Clar's sextet theory.^{1,2} This theory suggests that hexacene is more reactive than anthracene because of the gradual loss of benzenoid character.⁵ However, the more recent study carried out by Schleyer et al.⁹ indicates that the aromatic stabilization does not decrease along the acenes series, and the difference in reactivity depends on the aromaticity change of acenes during the reaction. In our previous study,¹⁰ the Diels–Alder reactivity of acenes with ethylene as well as its correlation with aromaticity were investigated and the results are in agreement with those of Schleyer et al.⁹ as well as in qualitative accord with available experimental data.¹¹

Singlet ($^1\Delta_g$) oxygen, or $^1\Delta_g-O_2$, takes part in many organic syntheses and biochemical processes to form peroxide and hydroperoxides.^{12–15} When it is present in the living cells, it reacts with lipid or unsaturated compounds to initiate the chain reactions leading to peroxidation, or it can react with xenobiotics to form superoxide anion radical and other active oxygen species of high cytotoxicity. The versatile reactivity of $^1\Delta_g-O_2$ is attributed to its electronic configuration.¹⁶ It includes a low-lying π^* LUMO, which makes $^1\Delta_g-O_2$ a good electrophile, and a high-energy π HOMO, which is orthogonal to the LUMO and supplies a certain amount of nucleophilicity. Due to the presence of a low-lying π^* LUMO, $^1\Delta_g-O_2$ may undergo many pericyclic reactions with unsaturated organic compounds. Indeed, the Diels–Alder reaction between $^1\Delta_g-O_2$ and various dienes has been known for many years.¹⁷ More recently, the reaction has found synthetic application for the stereocontrolled generation of two 1,4-related oxygen-bearing stereocenters.^{18,19}

The first observation of oxygen dissociated from endoperoxide (EPO) was made by Dufraisse et al. in 1926.²⁰ This reaction did not arouse much interest in the next several decades. In the late 1960s, Wasserman's work²¹ demonstrated that the oxygen evolved during thermolysis of 9,10-diphenylanthracene

EPO is in its singlet state, and the oxygen evolved is able to transfer to other photooxidizable substrates. A similar finding in photodissociations of aromatic EPOs has also been reported subsequently.²² Due to this important property, aromatic EPOs can be used in the development of highly reversible photochromic systems and as specific sources or traps of $^1\Delta_g-O_2$ in aqueous media.²³

According to a recent summary of reversible oxygen binding to aromatic compounds,²³ over 400 EPOs of hydrocarbons with one to nine fused benzenic cores have been reported in the literature.²⁴ Most of them were prepared by Diels–Alder reactions between $^1\Delta_g-O_2$ and the electron-rich carbon of the aromatic substrates. Interestingly, unsubstituted benzene and naphthalene fail to react with $^1\Delta_g-O_2$ and the corresponding EPOs must be prepared indirectly.²⁵ In 1974, the reactivity of the Diels–Alder reactions between $^1\Delta_g-O_2$ and various aromatic compounds, including anthracene, tetracene and pentacene, was measured by Stevens et al.²⁶ In 1980, a frontier molecular orbital²⁷ (FMO) study for these reactions was reported by Van den Heuvel et al.;²⁸ they established a correlation between the Hückel²⁹ FMO interactions and the experimental reaction rate constants of the Diels–Alder $^1\Delta_g-O_2$ addition to anthracene, tetracene and pentacene.

Similar to other Diels–Alder reactions, the addition reaction of $^1\Delta_g-O_2$ to acenes could proceed via two possible mechanisms.³⁰ It may take place in a concerted fashion, with partial formation of the two new bonds in the single transition state. If both bonds are formed exactly to the same extent in the transition state, the reaction is said to proceed via a synchronous concerted pathway; if the two new bonds are formed to different extents in the transition state, the pathway is asynchronous. The other mechanism involves a stepwise process: first an intermediate is formed with a single bond between the $^1\Delta_g-O_2$ (or $^3\Sigma_g-O_2$) and the acene and the subsequent formation of the second bond yields the cycloaddition product. The intermediate involved in the stepwise mechanism is a biradical. Thus this mechanism is expected to be energetically less favorable than the concerted one.³¹ Still, we might anticipate that the stepwise mechanism could compete favorably with the concerted pathway if the diene molecule is so sterically hindered as to effectively block the formation of the concerted transition state.^{32,33} However, this is unlikely to be the case for the acenes

* Corresponding author. Fax: (852)-2603-5057; Phone: (852)-2609-6281; E-mail: wkli@cuhk.edu.hk.

which have a planer structure. Clearly, for the reactions between ${}^1\Delta_g\text{-O}_2$ and acenes, both the energetic and steric factors favor the concerted mechanism. Indeed, this is the only pathway that will be investigated computationally in this work.

In the present work, we study the Diels–Alder reactivity of the acenes toward ${}^1\Delta_g\text{-O}_2$. The acenes studied include benzene, naphthalene, anthracene, tetracene and pentacene. The calculations were carried out at the G3(MP2) level,³⁴ and these calculated energetic quantities will be compared with the available experimental data.²⁶ Furthermore, an FMO study for the regioselectivity of these reactions will also be carried out, and a correlation between the FMO interaction and the G3(MP2) energy barriers will be established. Finally, the aromaticity of acenes and acenes adducts is evaluated by means of the nucleus independent chemical shifts (NICS) index,³⁵ which describes aromaticity from the magnetic point of view.

On the basis of the success of our previous G3(MP2) studies,^{36,37} the calculated results reported here may be regarded as reliable estimates for those structural and energetic quantities that have not been measured in experiment.

Methods of Calculation

The calculations in this study were carried out in a number of computing environments, including: a 20-node P4-Linux cluster, an IBM RS/6000 SP high performance computer cluster, a Hewlett-Packard Linux-based supercomputer provided by The Molecular Science Computing Facility High Performance Computing Center located at the Pacific Northwest National Laboratory. The Gaussian03 package³⁸ of programs was used in all Hartree–Fock and Møller–Plesset calculations, while the MOLPRO program³⁹ was used in the QCISD(T) single-point calculations. A complete-active-space multiconfiguration self-consistent field (CAS MCSCF) transition state (TS) search was carried out using the GAMESS⁴⁰ package of programs.

In this work, nine Diels–Alder reactions between ${}^1\Delta_g\text{-O}_2$ and five linear acenes are studied. These reactions involve 15 stable species (reactants and products) and nine TSs. Structural optimizations were calculated at the MP2(Full) and HF levels using the 6-31G(d) basis set. However, it should be noted that some of the TSs involved in the reaction of tetracene and pentacene could not be located at the MP2 and B3LYP levels. Also, the TSs structures found with the B3LYP functional may be erroneous; a fuller discussion on this point will be given later. In any event, for those TSs that were not found with the MP2(Full) method, they were identified at the HF/6-31G(d) level. Subsequent energetics calculations at the G3(MP2) level were carried out based on these structures.

All equilibrium structures were characterized by their harmonic vibrational frequency calculations at the HF/6-31G(d) level, yielding no imaginary frequency. On the other hand, each TS was characterized by its sole imaginary frequency and the vibrational normal mode with the imaginary frequency corresponds to the pathway of the ${}^1\Delta_g\text{-O}_2$ addition to acenes.

To establish the symmetry property of the TS, i.e., to determine if the two new C–O bonds are formed concomitantly, a CAS MCSCF search for the TS of the ${}^1\Delta_g\text{-O}_2$ addition reaction to naphthalene was carried out. It was found that the TS of this reaction is indeed structurally symmetric and thus the addition reactions between the ${}^1\Delta_g\text{-O}_2$ and acene are likely to proceed via the synchronous concerted mechanism. Additionally, it was also discovered that the electronic wave function of the TS is dominated by the ground-state configuration. These findings lend confidence to the results obtained in this work, all of which were obtained with the single-determinant approximation. Since

CAS MCSCF calculations are computationally intensive, the TS search for the ${}^1\Delta_g\text{-O}_2$ additions to the other acenes was not performed.

The energetics study of this work is based on the total energies computed at the G3(MP2) level,³⁴ which includes two single-point calculations at the MP2/G3MP2Large and QCISD(T)/6-31G(d) levels of theory, based on the structures optimized at the MP2(Full)/6-31G(d) level. In addition, there is a zero-point vibrational energy correction calculated at HF/6-31G(d) level, with a scaling factor of 0.8929, as well as an empirical high-level correction (HLC).

Since several TSs of the reactions involving tetracene and pentacene were only optimized at the HF/6-31G(d) level, the results of these reactions were denoted as G3(MP2)//HF in the following sections. On the other hand, the regular G3(MP2) results are called G3(MP2)//MP2.

Ground-state triplet ($X^3\Sigma_g$) oxygen, or $X^3\Sigma_g\text{-O}_2$, can be calculated directly. But direct calculation of ${}^1\Delta_g\text{-O}_2$ yields a much lower ${}^3\Sigma_g\rightarrow{}^1\Delta_g$ excitation energy,⁴¹ compared with the experimental value of 0.982 eV.⁴² Hence, in this work, to obtain the energy of ${}^1\Delta_g\text{-O}_2$ at the G3(MP2)//MP2 or G3(MP2)//HF level, we simply added the experimental excitation energy $\Delta E({}^3\Sigma_g\rightarrow{}^1\Delta_g)$ to the corresponding ground-state energies.

In the FMO theory, the second-order perturbation energy (ΔE) of Diels–Alder reaction results from the overlap between the orbitals on the “termini” of the diene and dienophile, and the dominant interaction in the early stage of the reaction is that between the HOMO of the diene and the LUMO of the dienophile. The quantity ΔE is calculated by the following expression:²⁸

$$\Delta E = E_{\text{LUMO}} - E_{\text{HOMO}} + \sqrt{(E_{\text{HOMO}} - E_{\text{LUMO}})^2 + 4\left(\frac{1}{\sqrt{2}}c_r - \frac{1}{\sqrt{2}}c_s\right)^2\beta_{\text{CO}}^2} \quad (1)$$

Here, c_r and c_s are the coefficients of the AOs on the terminal carbons r and s in the HOMO of the diene, and the factor $1/\sqrt{2}$ in front of c_r and c_s is the coefficient of LUMO of an isolated π -bond system, i.e., ${}^1\Delta_g\text{-O}_2$ in the present work. In this study, the HOMO of an acene and its energy (E_{HOMO}) were taken from ref 43, and they were calculated by the Hückel method; the energy of the LUMO of ${}^1\Delta_g\text{-O}_2$ (E_{LUMO}) is taken to be $\alpha + 0.22\beta$, where α is the Coulomb integral of the carbon atom and β is the resonance integral between two carbon p orbitals. Also, β_{CO} is the resonance integral between the p orbitals of carbon and oxygen atoms, and its value was taken to be 0.29β . All these parameters were obtained by fitting with experimental values, and they were reported by Van den Heuvel et al.²⁸ It should be noted that all ΔE values reported here have been divided by β . In other words, they are in unit of β .

For the study of the relative aromaticity of the acenes and acene adducts, NICS calculations were performed. The NICS index is defined as a negative value of the absolute shielding at the ring center, which can be computed by the GIAO method at the HF/6-31+G(d) theoretical level.³⁵ On the basis of the optimized structures obtained at the HF/6-31G(d) level, the aromatic ring are those ring with negative NICS value, and the more negative the index, the more aromatic the system. It should be pointed out that the 6-31+G(d) basis set has been recommended for NICS calculations, and NICS values are not very sensitive to the basis set used.³⁵

Results

In Figure 1, the structures of benzene (**1**), naphthalene (**2**), anthracene (**3**), tetracene (**4**), and pentacene (**5**) and those of

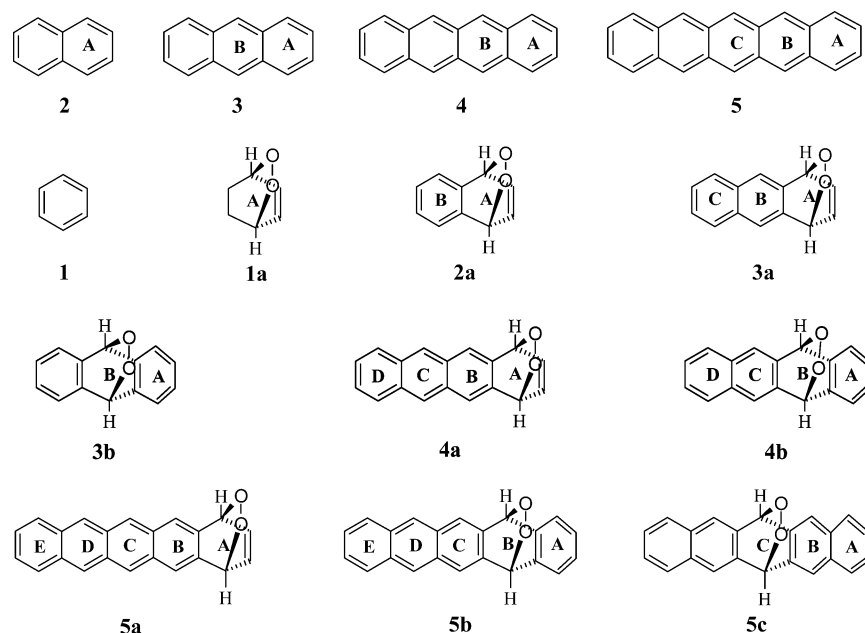


Figure 1. Labeling of the rings in the acenes and acene adducts studied in this work.

the nine acene adducts are also shown. In addition, the rings in the acenes are also labeled. The nine Diels–Alder reaction pathways between $^1\Delta_g$ -O₂ and acenes are displayed in Figure 2. Selected structural parameters (in Å and deg) and the imaginary frequencies for the nine TSs identified in this study are shown in Figure 3. The diagram shown in Figure 4 illustrates the FMO interactions in the Diels–Alder type reaction; the selected Hückel HOMO coefficients as well as the HOMO energy of the acenes are also given in this figure. The correlation between G3(MP2)//HF energy barriers and the ΔE s calculated from the FMO analysis is summarized in Figure 5.

In Table 1, the total energies calculated at the G3(MP2)//MP2 and G3(MP2)//HF levels for all species involved in this study are listed. In Table 2, the barriers and exothermicities of all nine reactions calculated at G3(MP2)//HF and G3(MP2)//MP2 levels are tabulated. Where available, experimental data are also included for comparison. The GIAO–SCF calculated NICS indices for the five acenes and nine acene adducts studied in this work are summarized in Table 3. In Table 4, the ΔE s of the reactions and the pertinent Hückel–HOMO parameters of acenes are given.

Discussion

Our discussion is divided into four parts: aromaticity, structures of the TSs, energetics of the reactions, and frontier molecular orbital study of the regioselectivity for the reactions between $^1\Delta_g$ -O₂ and acenes.

(i) Aromaticity and the NICS Indices. It should be mentioned that the NICS indices given in Table 3 for the linear acenes have already been reported in our previous work.¹⁰ As mentioned then, the center ring in the linear acenes is always the most aromatic one, and the aromaticity of the rings increases along the series $C > B > A$ (the labeling of the rings is given in Figure 1). Moreover, it is observed that the aromaticity of the center ring increases as the ring number increases. This finding has already been reported by Schleyer et al.,⁹ despite different theoretical methods were used in the geometry optimization.

As shown in Table 3, the aromaticity of reacted ring in the products decreases rapidly after the 1,4-oxygen addition to the acenes. The aromaticity change for the adjacent ring(s) depends on the position of the reacted ring in the acene: if the adjacent

ring is the outermost ring, it will become more aromatic. For example, the NICS index in the ring **A** of **5b** change from -3.9 to -10.0 . In other words, this ring becomes more aromatic. On the other hand, if the adjacent ring is not the outermost one, it will become less aromatic than before. For example, in **5b**, the value of ring **C** changes from -14.3 to -6.9 . Similar trends of aromaticity changes of acene adducts have been reported by Manoharan et al.⁴⁴ and they are also in agreement with the results of our previous work.¹⁰

In some earlier postulation, such as the sextet theory^{1,2,5} proposed by Clar, the reactivity increase for hexacene in comparison with anthracene is due to the loss of benzenoid character in hexacene. In contrast to this postulation, our results given in Table 3, going from naphthalene (**2**) to pentacene (**5**), the benzenoid character does not decrease, but it shifts from the outer ring to the inner one. These results are in agreement with Schleyer's study⁹ and our previous results.¹⁰

(ii) Structures of the Transition States. We now discuss the detailed structures of the nine TSs. At the HF level, all nine TSs were located. At the MP2 level, only six were found; the ones not identified were **4b-TS**, **5b-TS**, and **5c-TS**. These results are presented in Figure 3. As can be seen from this figure, all the TSs are structurally symmetric. That is to say, the two new C–O bonds are formed at the same time.

However, at the B3LYP level, the TSs optimized are not at all symmetric. For instance, in **4a-TS**, the two C \cdots O distances are found to be 1.880 and 2.303 Å. Similarly, the corresponding C \cdots O distance pairs for **4b-TS** and **5a-TS** are 2.316/2.410 and 1.887/2.360 Å, respectively. These TSs do not preserve the symmetry plane present in the reactants and products.

To ascertain the symmetry of the TSs, we performed a TS search for the reaction between $^1\Delta_g$ -O₂ and naphthalene using the high-level CAS MCSCF method. In previous CASSCF studies of $^1\Delta_g$ -O₂ Diels–Alder reactions by Leach and Houk¹⁶ and by Bobrowski et al.,⁴⁵ an active space consisting of 10 electrons and eight orbitals, (10,8), was suggested. This active space includes six orbitals, namely, σ_z , $(\pi_x = \pi_y)$, $(\pi_x = \pi_y)^*$, and σ_z^* , on the oxygen molecule (with eight electrons occupying the lower five orbitals in the ground state) and the HOMO–LUMO orbitals of the diene molecule (with two electrons occupying the HOMO in the ground state). For the aforemen-

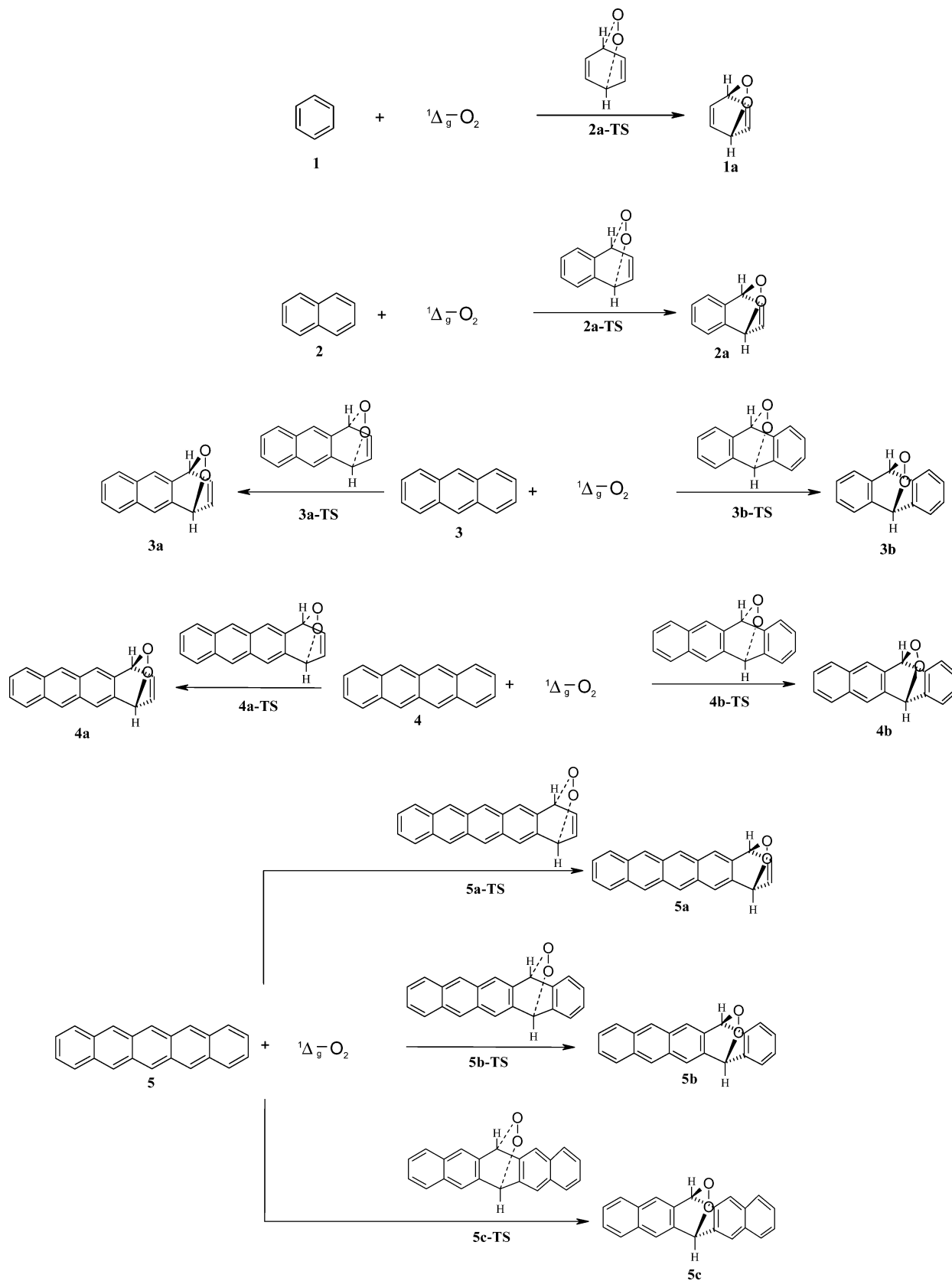


Figure 2. Reaction pathways between the acenes and singlet ($^1\Delta_g$) oxygen studied in this work.

tioned reaction between $^1\Delta_g$ -O₂ and naphthalene, we decided to use once again the 6-31G(d) basis set. For the active space we included 12 electrons and 12 orbitals. In other words, the level of theory adopted was CASSCF(12,12)/6-31G(d). We selected this larger active space because C₁ symmetry was assumed for the TS and all molecular orbitals have A₁ symmetry.

A larger active space can make sure that all orbitals which participate in the formation of the TS do not accidentally swap out of the active space during calculations. Such a precaution often ensures a smooth potential energy surface is obtained.

Upon carrying out the TS search for the reaction between $^1\Delta_g$ -O₂ and naphthalene at the CASSCF(12,12)/6-31G(d) level,

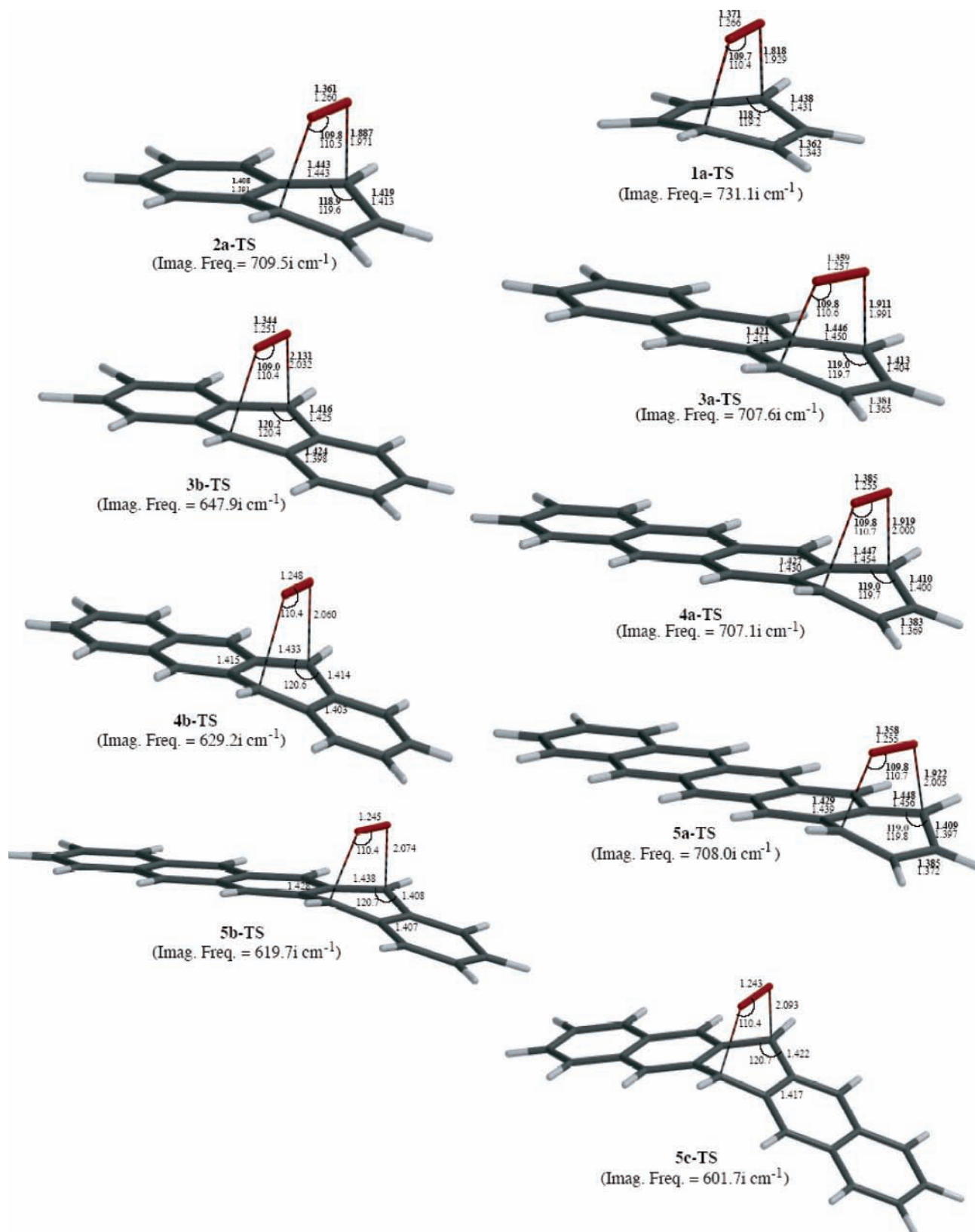


Figure 3. Optimized TSs of the reactions between the acenes and singlet ($^1\Delta_g$) oxygen with selected structural parameters (in Å and degrees). The MP2(Full)/6-31G(d) and HF/6-31G(d) values are given in bold font and normal font, respectively.

we found that the two C...O distances in this TS are 2.004 and 1.994 Å, which indicates the TS is essentially symmetric. Also, the TS obtained at this rather advanced level of theory is structurally very similar to those obtained with the HF and MP2 methods. Electronically, upon examining the mixing coefficients of the wave function, it was found that the ground-state

configuration (with a CI coefficient of 0.876, and the second largest coefficient is 0.111) dominates the ground-state wave function. These results support the symmetric TS as well as the results obtained with the single-determinant formalism. When we further extended the calculation to the CASSCF(16,14)/6-31G(d) level for the same TS search, very similar structural

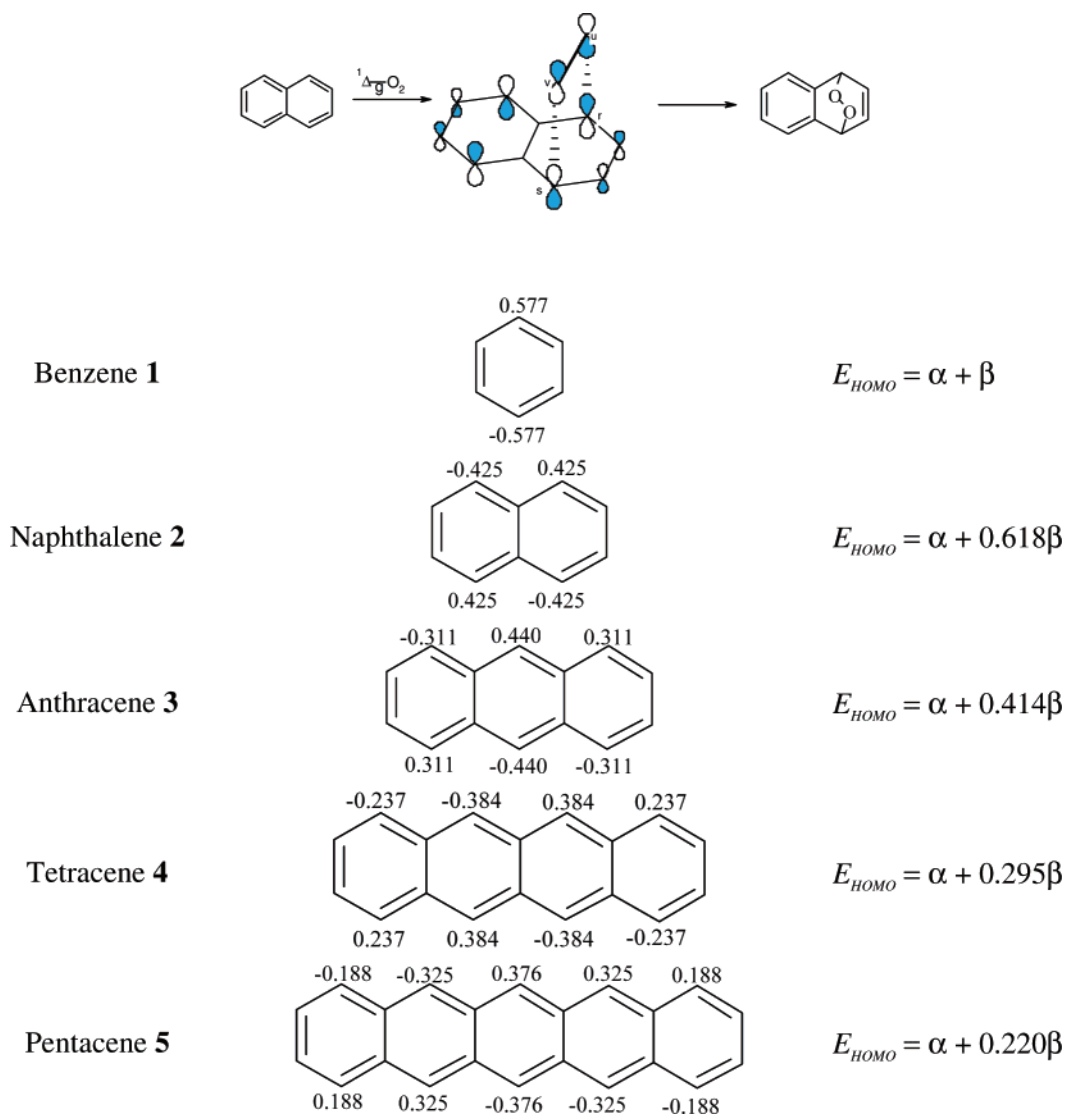


Figure 4. Illustration of the interaction between frontier molecular orbitals: selected orbital coefficients of Hückel–HOMO of linear acenes and the corresponding orbital energies.

results were obtained. Specifically, the two $\text{C}\cdots\text{O}$ distances in the TS become 2.007 and 1.997 Å. In other words, the TS once again is very nearly symmetric. Also, these results indicate that our first selected active space of (12,12) should be sufficient.

It should be mentioned that we also investigated the triplet oxygen addition pathways at various ab initio and DFT levels. However, we were unable to locate any TS which would lead to ring closure. This finding, along with our CAS MCSCF results, are in total accord with those obtained by Bobrowski et al.⁴⁵ for the 1,4-oxygen additions to butadiene and benzene using CAS MCSCF and CAS MCQDPT theories. These authors found that the reaction between $^1\Delta_g\text{-O}_2$ and benzene proceeds through a single-step mechanism with a symmetric transition state. A concerted TS was also found for the same reaction by Leach and Houk¹⁶ at the CASSCF(10,8)/6-31G(d) and CASSCF(12,10)/6-31G(d) levels of theory.

In the following discussion, we will mainly concentrate on the HF results presented in Figure 3, as HF/6-31G(d) is the only level at which all nine TSs are identified. In our previous study¹⁰ of the Diels–Alder reactions between ethylene and the acenes, we have shown that the $\text{C}\cdots\text{C}$ distances in the TSs between the ethylene and acene moieties is highly correlated with the aromaticity of the ring to be reacted. In this work, a very similar correlation is also observed.

The earliest TS of the 1,4-addition of oxygen to acenes has been found in **5c-TS**, the TS for the reaction between the center ring of pentacene and O_2 , which corresponds to a $\text{C}\cdots\text{O}$ distance of 2.093 Å. On the other hand, the latest TS has been found at **1a-TS**, the TS for the reaction between benzene and O_2 , in which the $\text{C}\cdots\text{O}$ distance is 1.929 Å.

Similar to our previous study,¹⁰ the dienophile addition to the center ring of an acene has a longer $\text{C}\cdots\text{O}$ distance in the TS (i.e., an earlier TS) than the other rings. As shown in Figure 3, the $\text{C}\cdots\text{O}$ distances for **5a-TS**, **5b-TS**, and **5c-TS** are found to be 2.005, 2.074 and 2.093 Å, respectively; in **3a-TS** and **3b-TS**, the $\text{C}\cdots\text{O}$ distances calculated are 1.991 and 2.032 Å, respectively. The $\text{C}\cdots\text{O}$ distances in the TSs which have not been discussed are 1.971, 2.000, and 2.060 Å in **2a-TS**, **4a-TS** and **4b-TS**, respectively. These results are also in accord with the aforementioned trends. Among the nine TSs found in this work, there is a correlation between the $\text{C}\cdots\text{O}$ distances in the TSs and the aromaticity of the rings in the acenes: the more aromatic the ring in an acene, the earlier the TS.

Before proceeding to the next section, it is mentioned that, by the assumption of a symmetrical and concerted TS for the reactions studied, a very good correlation is found between the G3(MP2)//HF energy barriers and the ΔE s calculated from FMO analysis. Moreover, as will be discussed in section iii, these

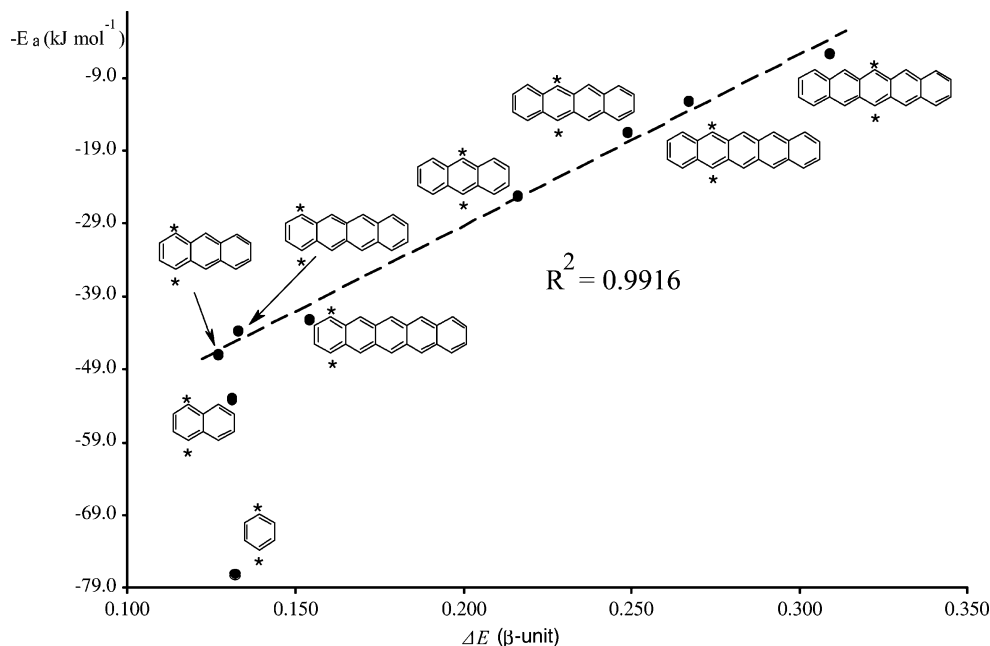


Figure 5. Correlation between the G3(MP2)//HF barriers (E_a) and the second-order perturbation energy (ΔE). The positions attacked by singlet oxygen are indicated by asterisks.

results are also in agreement with available experimental data.^{26,28} Such an accord supports the symmetric TS model and the use of single-determinant theories in the present work. A detailed discussion of the FMO analysis will be given in section iv.

(iii) The Energetics of the Reactions between Singlet Oxygen and the Acenes. Examining the reaction barriers and exothermicities listed in Table 2, among the nine reactions studied in this work, the reaction of **5c** has the largest exothermicity ($-179.1 \text{ kJ mol}^{-1}$) and the smallest energy barrier (5.7 kJ mol^{-1}); this reaction corresponds to the 1,4-addition to the center ring of pentacene (**5**). In other words, this is the most energetically favored reaction in this study. In **5**, the center ring is the most aromatic as well as the most reactive. Its neighboring rings are less aromatic as well as less reactive (for the reaction of **5b**, the exothermicity is $-161.9 \text{ kJ mol}^{-1}$ and the barrier is 12.1 kJ mol^{-1}). Finally, the outermost rings are least aromatic and least reactive; the exothermicity and energy barrier for the reaction of **5a** are -87.0 and 42.2 kJ mol^{-1} , respectively. In the experiment by Stevens et al.,²⁶ the energy barrier for the reaction of **5c** has been taken as the reference for the measurements of other reaction barriers, and it was taken to be 0.0 kJ mol^{-1} in their paper. For the sake of easy comparison, our G3(MP2)//HF calculated energy barrier for this reaction will be taken as the experimental value in the following comparison.

A very similar trend is also found in the other reactions. For anthracene, reaction of **3b** (with an exothermicity of $-123.8 \text{ kJ mol}^{-1}$ and a barrier of 25.2 kJ mol^{-1}) is favored over reaction of **3a**, (with an exothermicity of $-73.8 \text{ kJ mol}^{-1}$ and a barrier of 46.9 kJ mol^{-1}). Once again, the center ring of anthracene is the most aromatic as well as most reactive. The reported experimental energy barrier of the reaction of **3b** is 25.5 kJ mol^{-1} higher than that of the reaction of **5c**.²⁶ Our G3(MP2)//HF results show that the barrier of the reaction of **3b** is 19.5 kJ mol^{-1} higher than that of the reaction of **5c**. So our calculated results are in fairly good agreement with experiment.

Similarly, for tetracene, the reaction of **4b** is the most energetically favored: its exothermicity and barrier are -149.8 and 16.4 kJ mol^{-1} , respectively. Meanwhile, the reaction of **4a** has an exothermicity of $-82.9 \text{ kJ mol}^{-1}$ and a barrier of 43.7

kJ mol^{-1} . The experimental energy barrier for the reaction of **4b** is 14.6 kJ mol^{-1} higher than that of the reaction of **5c**.²⁶ This value is once again in good agreement with our G3(MP2)//HF result of 10.7 kJ mol^{-1} .

To summarize, along the series of linear acenes from benzene to pentacene, the reactivity toward singlet oxygen addition increases in the order of benzene (**1**) < naphthalene (**2**) < anthracene (**3**) < tetracene (**4**) < pentacene (**5**). The aromaticity of the acenes also increases in the same order. A similar trend or correlation was our found in our previous work on the reactions between acenes and ethylene.¹⁰

A possible explanation of this correlation has been discussed previously,¹⁰ so only a brief discussion will be given here. A natural bond orbital (NBO) study⁴⁶ shows that acene has a highly delocalized structure, and the four carbon atoms next to the meso-carbons of the inner ring are electron-deficient. Therefore, the addition of dieneophile such as ethylene and singlet oxygen to meso-carbons at the inner ring results in reduction of electron deficiency for the other four carbon atoms in the ring.

On the basis of the reactivity index measured from the quantum yield of photoperoxidation in air-saturated solutions of benzene at $25 \text{ }^\circ\text{C}$, the rate constants for the addition reactions of $^1\Delta_g\text{-O}_2$ to with anthracene, tetracene and pentacene have been reported by Stevens et al.²⁶ The measured rates (in $\text{M}^{-1} \text{ s}^{-1}$) of the reactions involving anthracene, tetracene and pentacene are 0.15×10^{-6} , 14×10^{-6} , and 4200×10^{-6} , respectively. Aromatic systems such as benzene and naphthalene are unreactive with $^1\Delta_g\text{-O}_2$, but with the highly reactive dicyanoacetylene they give [4 + 2] cycloadducts.¹¹ These findings are in (qualitative) accord with the aforementioned trend of reactivity calculated in the present work.

Our calculated results are also indirectly supported by another experimental evidence. In 1979, Biermann and Schmidt studied the Diels–Alder reactivity of polycyclic aromatic hydrocarbons.⁵ They measured the rates of reaction of 21 acene-type hydrocarbons with excess maleic anhydride at $91.5 \text{ }^\circ\text{C}$ in 1,2,4-trichlorobenzene. They found that anthracene, tetracene, and pentacene, among others, react cleanly under these conditions, while benzene and naphthalene show no noticeable Diels–Alder reactivity. The measured second-order rate constants (in L M^{-1}

TABLE 1: Total Energies (in hartree) of the Stationary Points for the Diels–Alder Reactions between Acenes 1–5 and Singlet ($^1\Delta_g$) Oxygen

species	symmetry	G3(MP2)//MP2 ^a	G3(MP2)//HF ^b
Reactant			
(triplet O ₂) $^3\Sigma_g^-$ -O ₂	$D_{\infty h}$	-150.16434	-150.16380
(singlet O ₂) ^c $^1\Delta_g$ -O ₂	$D_{\infty h}$	-150.12825	-150.12771
benzene 1	D_{6h}	-231.82976	-231.82856
naphthalene 2	D_{2h}	-385.21410	-385.21203
anthracene 3	D_{2h}	-538.59271	-538.58972
tetracene 4	D_{2h}	-691.96892	-691.96484
pentacene 5	D_{2h}	-854.34436	-845.33862
Product			
1a	C_{2v}	-381.96061	-381.95666
2a	C_s	-535.36511	-535.36047
3a	C_s	-688.75116	-688.74554
3b	C_{2v}	-688.76965	-688.76458
4a	C_s	-842.13080	-842.12414
4b	C_s	-842.15558	-842.14959
5a	C_s	-995.50732	-995.49945
5b	C_s	-995.53516	-995.52801
5c	C_{2v}	-995.54144	-995.53454
Transition State			
1-TS	C_{2v}	-381.93417	-381.92694
2a-TS	C_s	-535.32696	-535.31927
3a-TS	C_s	-688.70831	-688.69958
3b-TS	C_{2v}	-688.71191	-688.70782
4a-TS	C_s	-842.08600	-842.07592
4b-TS	C_s		-842.08630
5a-TS	C_s	-995.46173	-995.45025
5b-TS	C_s		-995.46173
5c-TS	C_{2v}		-995.46417
Reactants			
1 + $^1\Delta_g$ -O ₂		-381.95801	-381.95627
2 + $^1\Delta_g$ -O ₂		-535.34235	-535.33974
3 + $^1\Delta_g$ -O ₂		-688.72096	-688.71743
4 + $^1\Delta_g$ -O ₂		-842.09717	-842.09255
5 + $^1\Delta_g$ -O ₂		-995.47261	-995.46633

^a Standard G3(MP2) procedure, where molecular geometry is optimized at MP2(Full)/6-31 G(d); zero-point correction is based on the frequencies calculated at the HF/6-31G(d) level. ^b Modified G3(MP2) procedure, in which both molecular geometry and zero-point vibration correction are calculated at the HF/6-31 G(d) level. ^c Total energy of singlet O₂ is calculated by the addition of experimental excitation energies, $\Delta E(^3\Sigma_g^- \rightarrow ^1\Delta_g)$, to the calculated total energy of triplet O₂. Excitation energy $\Delta E(^3\Sigma_g^- \rightarrow ^1\Delta_g)$ is taken to be 0.03069 hartree (0.982 eV), according to ref 38.

TABLE 2: Energy Barriers and Exothermicities (in kJ mol⁻¹) of the Reactions between Acenes 1 to 5 and Singlet ($^1\Delta_g$) Oxygen Calculated at the G3(MP2)//MP2 and G3(MP2)//HF Levels

reaction product	G3(MP2)//MP2		G3(MP2)//HF ^a	
	barrier	exothermicity	barrier	exothermicity
1	62.6	-7.6	77.0	-1.0
2	40.4	-59.8	53.7	-54.4
3a	33.2	-79.3	46.9	-73.8
3b	23.8	-127.8	25.2 (25.5) ^b	-123.8
4a	29.3	-88.3	43.7	-82.9
4b		-153.4	16.4 (14.6) ^b	-149.8
5a	28.6	-91.1	42.2	-87.0
5b		-164.2	12.1	-161.9
5c		-180.1	5.7 (0.0) ^{b,c}	-179.1

^a G3(MP2)//HF quantities calculated based on the structural optimization at HF/6-31G(d) level. ^b Experimental barriers, relative to the energy barrier for the reaction of **5c**, reported in ref 26. ^c This energy was taken as the reference for the measurement of other energy barriers in ref 26.

s⁻¹) of the reactions involving anthracene, tetracene and pentacene are 2.27×10^{-3} , 9.42×10^{-2} , and 1.64, respectively.

TABLE 3: NICS Indices (in ppm) for the Acenes and Acene Adducts

species	ring	point group	NICS 6-31+G(d) ^a	NICS 6-31+G(d) ^b
benzene 1		D_{6h}	-9.7	-9.7
1a		C_{2v}	-3.1	
naphthalene 2		D_{2h}	-9.5	-10.0
2a		C_s		
ring with O ₂	A		-1.4	
ring without O ₂	B		-10.0	
anthracene 3		D_{2h}		
outer ring			-7.4	-8.3
central ring			-13.1	-13.3
3a		C_s		
ring with O ₂	A		-1.7	
central ring	B		-10.0	
outer ring	C		-11.3	
3b		C_{2v}		
outer ring	A		-10.0	
ring with O ₂	B		-0.3	
tetracene 4		D_{2h}		
outer ring	A		-5.5	-6.8
central ring	B		-12.7	-13.1
4a		C_s		
ring with O ₂	A		-1.3	
central ring	B		-6.7	
central ring	C		-12.8	
outer ring	D		-8.0	
4b		C_s		
outer ring	A		-10.0	
ring with O ₂	B		0.01	
central ring	C		-9.2	
outer ring	D		-9.9	
pentacene 5		D_{2h}		
outer ring	A		-3.9	-5.5
middle ring	B		-11.2	-12.0
central ring	C		-14.3	-14.3
5a		C_s		
ring with O ₂	A		-1.4	
middle ring	B		-4.8	
central ring	C		-11.9	
middle ring	D		-13.0	
outer ring	E		-6.0	
5b		C_s		
outer ring	A		-10.0	
ring with O ₂	B		0.0	
central ring	C		-6.9	
middle ring	D		-12.9	
outer ring	E		-8.9	
5c		C_{2v}		
outer ring	A		-9.9	
middle ring	B		-9.3	
ring with O ₂	C		0.3	

^a HF/6-31+G(d) NICS calculations based on the HF/6-31G(d) structures. ^b NICS values based on the B3LYP/6-31G(d) structures reported in ref 10.

TABLE 4: Second-Order Perturbation Energy (ΔE , in β -Unit) of the Reactions between Acenes and Singlet Oxygen ($^1\Delta_g$) Calculated by Hückel Molecular Orbital (HMO) Theory and Pertinent HMO Parameters for the HOMO of Acenes

acene	aromatic ring attacked by $^1\Delta_g$ -O ₂					
	A		B		C	
	ΔE	$(c_r - c_s)^2$	ΔE	$(c_r - c_s)^2$	ΔE	$(c_r - c_s)^2$
1	0.132	1.332				
2	0.131	0.723				
3	0.127	0.378	0.216	0.774		
4	0.133	0.225	0.249	0.590		
5	0.154	0.141	0.267	0.423	0.309	0.566

Additionally, they found that the most reactive positions of the linear acenes are the meso-carbons of the inner ring in each

acene. While these reactions do not involve the addition of singlet oxygen, the kinetics results are in accord with the computational results reported here. Hence, we may take these experimental data as indirect evidence that support our G3(MP2) results.

(iv) Frontier Molecular Orbital Study of Regioselectivity.

As mentioned before, Van den Heuvel et al. reported that the ΔE calculated in a FMO analysis is well correlated with experimental rate constants for the reactions between $^1\Delta_g\text{-O}_2$ and acenes, including anthracene, tetracene and pentacene.²⁸ In the present work, we employed the FMO analysis to study the regioselectivity of these reactions.

In Table 4, the largest ΔE of the reactions between $^1\Delta_g\text{-O}_2$ and pentacene is the one for **5c** (0.309 β -unit), the second is that of **5b** (0.267 β -unit), and the one for **5a** has the smallest value (0.154 β -unit); this trend is in line with the calculated G3(MP2)//HF reaction barriers of these reactions. Similarly, the ΔE of **4b** (0.249 β -unit) is larger than that of **4a** (0.133 β -unit), and the ΔE of **3b** (0.216 β -unit) is larger than that of **3a** (0.127 β -unit). These results have led us to believe that FMO analysis can be used to study the regioselectivity of the reactions between $^1\Delta_g\text{-O}_2$ and acenes.

Van den Heuvel's work²⁸ has shown that ΔE is proportional to natural log of the rate constant k . Thus, ΔE should also be proportion to the negative value of the energy barrier for the reaction. This relationship is now shown in Figure 5. Except for the ΔE s of the reactions involving benzene and naphthalene, 0.132 and 0.131 β -unit, respectively, for which the G3(MP2)//HF energy barriers are higher than the FMO predicted values, the ΔE s of the remaining seven reactions are well correlated ($R^2 = 0.9916$) with the negative value of the G3(MP2)//HF energy barriers.

Since concerted reactions pathway has been assumed in the FMO model used in the present studies, the present analysis supports the conclusion that the TS is symmetric for the $^1\Delta_g\text{-O}_2$ additions to the acenes.

Conclusions

In this work, the reactivity of five acenes, including benzene, naphthalene, anthracene, tetracene, and pentacene, toward the 1,4-addition of singlet oxygen has been studied using the high-level ab initio model of G3(MP2). It is seen that all nine reactions are exothermic and concerted, and the most favorable reaction pathway is the reaction to yield **5c**, with $^1\Delta_g\text{-O}_2$ added to the center ring of pentacene. Also, the reactivity of acenes increases with the number of rings in the molecule. These findings are in good agreement with frontier molecular orbital analysis. For each acene, the most reactive sites of reaction are the meso-carbons of the center ring. Correlating these results with the NICS values of the rings of an acene, it is found that, the most reactive ring of an acene is also the most reactive one. A brief rationalization of this correlation is given. These computational results are in good accord with the available experimental kinetics data.

Acknowledgment. This work was supported by a grant from the Research Grants Council of the Hong Kong Special Administrative Region (Project No. CUHK4275/00P). The authors are grateful to an anonymous donor who made a donation to the Department of Chemistry at the Chinese University of Hong Kong. The generous allocation of computer time on the IBM RS/6000 SP High Performance Computer Cluster in the Computer Service Center at the Chinese University of Hong Kong is much appreciated. S.H.C. wishes to thank

Dr. Adam Liwo for helpful discussions. This research was performed in part using the Molecular Science Computing Facility (MSCF) in the William R. Wiley Environmental Molecular Sciences Laboratory, a national scientific user facility sponsored by the U.S. Department of Energy's Office of Biological and Environmental Research and located at the Pacific Northwest National Laboratory. Pacific Northwest is operated for the U.S. Department of Energy by Battelle. The authors would like to thank the referees for their constructive comments. They are also grateful to Professor Peter Gill at the Australian National University for helpful discussions.

References and Notes

- (1) Clar, E. *Polycyclic Hydrocarbons*, Academic Press: London, 1964.
- (2) Clar, E. *The Aromatic Sextet*, Wiley: London, 1972.
- (3) *Handbook of Polycyclic Aromatic Hydrocarbons*; Bjorseth, A. Ed.; Dekker: New York, 1983.
- (4) *Polynuclear Aromatic Hydrocarbons: A Decade of Progress*; Cooke, M., Dennis, A. J., Eds.; Battelle Press: Columbus, OH, 1988.
- (5) Biermann, D.; Schmidt, W. J. *J. Am. Chem. Soc.* **1980**, *102*, 3163.
- (6) Biermann, D.; Schmidt, W. J. *J. Am. Chem. Soc.* **1980**, *102*, 3173.
- (7) Harvey, R. G. *Polycyclic Aromatic Hydrocarbons*; Wiley-VCH: New York, 1997.
- (8) Suresh, C. H.; Gadre, S. R. *J. Org. Chem.* **1999**, *64*, 2505.
- (9) Schleyer, P. v. R.; Manoharan, M.; Jiao, H.; Stahi, F. *Org. Lett.* **2001**, *3*, 3643.
- (10) Cheng, M.-F.; Li, W.-K. *Chem. Phys. Lett.* **2002**, *368*, 630.
- (11) Ciganek, E. *Tetrahedron Lett.* **1967**, *34*, 3321.
- (12) Halliwell, B.; Gutteridge, J. M. C. *Free Radicals in Biology and Medicine*; Clarendon Press: Oxford, U.K., 1985.
- (13) Kearns, D. R. *Chem. Rev.* **1971**, *71*, 395.
- (14) Lissi, E. A.; Encinas, M.; Lemp, E.; Rubio, M. A. *Chem. Rev.* **1993**, *93*, 699.
- (15) *Free Radicals in Biology*; Pryor, W. A. Ed.; Academic Press: New York, 1982; Vol. V.
- (16) Leach, A. G.; Houk, K. N. *Chem. Commun.* **2002**, 1243.
- (17) Windaus, A.; Brunken, J. *Liebigs Ann. Chem.* **1928**, *103*, 225.
- (18) Zhou, G.; Gao X.; Li, W. Z.; Li, Y. *Tetrahedron Lett.* **2001**, *42*, 3101.
- (19) Kusama, H.; Hara, R.; Kawahara, S.; Nishimori, T.; Kashima, H.; Nakamura, N.; Morihira, K.; Kuwajima, I. *J. Am. Chem. Soc.* **2002**, *122*, 3811.
- (20) Moureu, C.; Dufraisse, C.; Dean, P. M. *C. R. Acad. Sci.* **1926**, *182*, 1584.
- (21) Wasserman, H. H.; Scheffer, J. R. *J. Am. Chem. Soc.* **1967**, *89*, 3073.
- (22) (a) Schmidt, R.; Drews, W.; Brauer, H.-D. *J. Am. Chem. Soc.* **1980**, *102*, 2791. (b) Rigaudy, J.; Breliere, C.; Scribe, P. *Tetrahedron Lett.* **1978**, *7*, 687.
- (23) Aubry, J.-M.; Pierlot C.; Rigaudy J.; Schmidt, R. *Acc. Chem. Res.* **2003**, *36*, 668.
- (24) Bloodworth, A. J.; Eggelte H. J. In *Singlet O₂*; Frimer, A. A., Ed.; CRC Press: Boca Raton, FL, 1985; Vol. II, Chapter 4.
- (25) (a) Noh, T.; Gan, H.; Halfon, S.; Hrnjez, B. J.; Yang, N. C. *J. Am. Chem. Soc.* **1997**, *119*, 7470. (b) Schäfer-Ridder, M.; Brocker, U.; Vogel, E. *Angew. Chem., Int. Ed. Engl.* **1976**, *15*, 228.
- (26) Stevens, B.; Perez, S. R.; Ors, J. A. *J. Am. Chem. Soc.* **1974**, *96*, 6846.
- (27) Fleming, I. *Frontier Orbitals and Organic Chemical Reactions*; John Wiley and Sons: New York, 1978.
- (28) Van den Heuvel, C. J. M.; Verhoeven, J. W.; de Boer, Th. J. *J. R. Neth. Chem. Soc.* **1980**, *9*, 280.
- (29) Liberles, A. *Introduction to Molecular-Orbital Theory*; Holt, Rinehart and Winston: New York, 1966.
- (30) Houk, K. L.; González, J.; Li, Y. *Acc. Chem. Res.* **1995**, *28*, 81.
- (31) Orlova, G.; Goddard J. D. *J. Org. Chem.* **2001**, *66*, 4026.
- (32) Wiest, O.; Montiel, D. C.; Houk, K. N. *J. Phys. Chem. A* **1997**, *101*, 8378.
- (33) Chen, J. S.; Houk, K. N.; Foote, C. S. *J. Am. Chem. Soc.* **1998**, *120*, 12303.
- (34) Curtiss, L. A.; Redfern P. C.; Raghavachari K.; Rassolov V.; Pople, J. A. *J. Chem. Phys.* **1999**, *110*, 4703.
- (35) Schleyer, P. v. R.; Maerker, C.; Dransfeld, A.; Jiao, H.; Hommes, N. J. R. v. E. *J. Am. Chem. Soc.* **1996**, *118*, 6317.
- (36) Ma, N. L.; Lau, K.-C.; Chien S.-H.; Li, W.-K. *Chem. Phys. Lett.* **1999**, *311*, 275.
- (37) Chien, S.-H.; Li, W.-K.; Ma, N. L. *J. Phys. Chem. A* **2000**, *104*, 11398.

- (38) Gaussian 03, Revision B.05. Frisch, M. J.; Trucks, G. W.; Schlegel, H. B.; Scuseria, G. E.; Robb, M. A.; Cheeseman, J. R.; Montgomery, J. A., Jr.; Vreven, T.; Kudin, K. N.; Burant, J. C.; Millam, J. M.; Iyengar, S. S.; Tomasi, J.; Barone, V.; Mennucci, B.; Cossi, M.; Scalmani, G.; Rega, N.; Petersson, G. A.; Nakatsuji, H.; Hada, M.; Ehara, M.; Toyota, K.; Fukuda, R.; Hasegawa, J.; Ishida, M.; Nakajima, T.; Honda, Y.; Kitao, O.; Nakai, H.; Klene, M.; Li, X.; Knox, J. E.; Hratchian, H. P.; Cross, J. B.; Bakken, V.; Adamo, C.; Jaramillo, J.; Gomperts, R.; Stratmann, R. E.; Yazyev, O.; Austin, A. J.; Cammi, R.; Pomelli, C.; Ochterski, J. W.; Ayala, P. Y.; Morokuma, K.; Voth, G. A.; Salvador, P.; Dannenberg, J. J.; Zakrzewski, V. G.; Dapprich, S.; Daniels, A. D.; Strain, M. C.; Farkas, O.; Malick, D. K.; Rabuck, A. D.; Raghavachari, K.; Foresman, J. B.; Ortiz, J. V.; Cui, Q.; Baboul, A. G.; Clifford, S.; Cioslowski, J.; Stefanov, B. B.; Liu, G.; Liashenko, A.; Piskorz, P.; Komaromi, I.; Martin, R. L.; Fox, D. J.; Keith, T.; Al-Laham, M. A.; Peng, C. Y.; Nanayakkara, A.; Challacombe, M.; Gill, P. M. W.; Johnson, B.; Chen, W.; Wong, M. W.; Gonzalez, C.; Pople, J. A. Gaussian, Inc.: Wallingford, CT, 2004.
- (39) MOLPRO, a package of ab initio programs. Werner, H.-J.; Knowles, P. J.; Schütz, M.; Lindh, R.; Celani, P.; Korona, T.; Rauhut, G.; Manby, F. R.; Amos, R. D.; Bernhardsson, A.; Berning, A.; Cooper D. L., Deegan, M. J. O.; Dobbyn, A. J.; Eckert, F.; Hampel, C.; Hetzer, G.; Lloyd, A. W.; McNicholas, S. J.; Meyer, W.; Mura, M. E.; Nicklass, A.; Palmieri, P.; Pitzer, R.; Schumann, U.; Stoll, H.; Stone A. J.; Tarroni R.; Thorsteinsson, T.
- (40) Schmidt, M. W.; Baldridge, K. K.; Boatz, J. A.; Elebert, S. T.; Gordon, M. S.; Jensen, J. H.; Koseki, S.; Matsunaga, N.; Nguyen, K. A.; Su, S. J.; Windus, T. L.; Dupuis, M.; Montgomery, J. A. *J. Comput. Chem.* **1993**, *14*, 1347.
- (41) The ${}^3\Sigma_g^- \rightarrow {}^1\Delta_g$ excitation energies of O₂ calculated at the G3(MP2)//MP2 and G3(MP2)//HF levels are 0.405 and 0.395 eV, respectively.
- (42) Miura, N.; Kenro, H.; Takahashi, K.; Taniguchi, N.; Matsumi, Y. *J. Chem. Phys.* **2002**, *116*, 5551.
- (43) Straub, H. *Hückel Molecular Orbitals*; Springer-Verlag: Berlin, 1996.
- (44) Manoharan, M.; Proft, F. D.; Greelings, P. *Perkin Trans. 2* **2000**, 1767.
- (45) Bobrowski, M.; Liwo, A.; Oldziej, S.; Jeziorek, D.; Ossowski, T. *J. Am. Chem. Soc.* **2000**, *122*, 8112.
- (46) Reed, A. E.; Curtiss L. A.; Weinhold, F. *Chem. Rev.* **1988**, *88*, 899.